Journal of Inorganic Biochemistry 180 (2018) 211–221

Contents lists available at ScienceDirect

Journal of Inorganic Biochemistry

journal homepage: www.elsevier.com/locate/jinorgbio

Binding of vanadium to human serum transferrin - voltammetric and spectrometric studies

Cristina G. Azevedo[a], Isabel Correia[a], Margarida M.C. dos Santos[a,*], Marino F.A. Santos[a,b], Teresa Santos-Silva[b], James Doutch[c], Luz Fernandes[b,d], Hugo M. Santos[b,d], José L. Capelo[b,d], João Costa Pessoa[a,*]

[a] Centro de Química Estrutural, Instituto Superior Técnico, Universidade de Lisboa, Av. Rovisco Pais, 1049-001 Lisboa, Portugal
[b] UCIBIO, REQUIMTE, Departamento de Química, Faculdade de Ciências e Tecnologia, Universidade Nova de Lisboa, 2829-516 Caparica, Portugal
[c] ISIS Pulsed Neutron and Muon Source, Science and Technology Facilities Council, Harwell Science and Innovation Campus, Didcot OX11 0QX, UK
[d] PROTEOMASS Scientific Society, Madan Park, Rua dos Inventores, 2825-152 Caparica, Portugal

ARTICLE INFO

Keywords:
Vanadium
Transferrin
Voltammetric studies
MALDI-TOF
SAXS
Binding constants

ABSTRACT

Previous studies generally agree that in the blood serum vanadium is transported mainly by human serum transferrin (hTF). In this work through the combined use of electrochemical techniques, matrix-assisted laser desorption/ionization time of flight (MALDI-TOF) mass spectrometry and small-angle X-ray scattering (SAXS) data it is confirmed that both V^{IV} and V^{V} bind to apo-hTF and holo-hTF. The electrochemical behavior of solutions containing vanadate(V) solutions at pH = 7.0, analyzed by using two different voltammetric techniques, with different time windows, at a mercury electrode, Differential Pulse Polarography (DPP) and Cyclic Voltammetry (CV), is consistent with a stepwise reduction of $V^{V} \rightarrow V^{IV}$ and $V^{IV} \rightarrow V^{II}$. Globally the voltammetric data are consistent with the formation of 2:1 complexes in the case of the system V^{V}-apo-hTF and both 1:1 and 2:1 complexes in the case of V^{V}-holo-hTF; the corresponding conditional formation constants were estimated. MALDI-TOF mass spectrometric data carried out with samples of $V^{IV}OSO_4$ and apo-hTF and of $NH_4V^{V}O_3$ with both apo-hTF and holo-hTF with V:hTF ratios of 3:1 are consistent with the binding of vanadium to the proteins. Additionally the SAXS data suggest that both $V^{IV}OSO_4$ and $NaV^{V}O_3$ can effectively interact with human apo-transferrin, but for holo-hTF no clear evidence was obtained supporting the existence or the absence of protein-ligand interactions. This latter data suggest that the conformation of holo-hTF does not change in the presence of either $V^{IV}OSO_4$ or $NH_4V^{V}O_3$. Therefore, it is anticipated that V^{IV} or V^{V} bound to holo-hTF may be efficiently uptaken by the cells through receptor-mediated endocytosis of hTF.

1. Introduction

Human serum transferrin (hTF) is the primarily transporter of Fe^{III} ions in the blood. It contains around 630 amino acids arranged in two similar lobes: the N-terminal (hTF_N) and the C-terminal (hTF_C) lobes. Each lobe can reversibly bind a Fe^{III} ion, but also other metal ions [1] [2] [3]. Conformational changes take place upon binding or release of Fe^{III} ions: in the apo-form (apo-hTF) the protein is in the 'open conformation', while upon binding two Fe^{III} ions, forming what we may designate as $(Fe)_2$hTF (holo-hTF), the protein adopts a structure which is often designated by 'closed conformation'. This conformation is recognized by the hTF receptors located at the surface of cells, iron uptake occurring by internalization of transferrin through a receptor-mediated 'endocytosis' process.

The ability of transferrin to bind Fe^{III} and other metal ions depends on the pH [1] [4] and previous studies globally agree that in the blood serum vanadium is transported mainly bound to transferrin [5] [6] [7] [8] [9] [10] [11] [12]. In the whole blood, for relatively high amounts of vanadium a significant part may be bound to erythrocytes (red blood cells) [13] [14] [15], most probably as V^{IV} [16] [17]; however, for the concentrations normally found in the blood of humans treated with vanadium compounds (e.g. $V^{IV}O(carrier)_n$, where carrier is the ligand present in the V-compound), ca. up to 1–5 μM [18] [19], vanadium is bound to hTF not including the carrier ligand [6] [12] [20] [21] [22] [23] [24]. In aqueous solutions, there is a global tendency for vanadium to be in the V^{V} oxidation state. For example, Chasteen et al. [25] reported that oxidovanadium(IV) ($V^{IV}O^{2+}$) is very susceptible to aerobic oxidation, and the pH-sensitive half-life for the oxidation is estimated

* Corresponding authors.
E-mail address: joao.pessoa@ist.utl.pt (J.C. Pessoa).

https://doi.org/10.1016/j.jinorgbio.2017.12.012
Received 16 October 2017; Received in revised form 20 November 2017; Accepted 19 December 2017
Available online 26 December 2017
0162-0134/

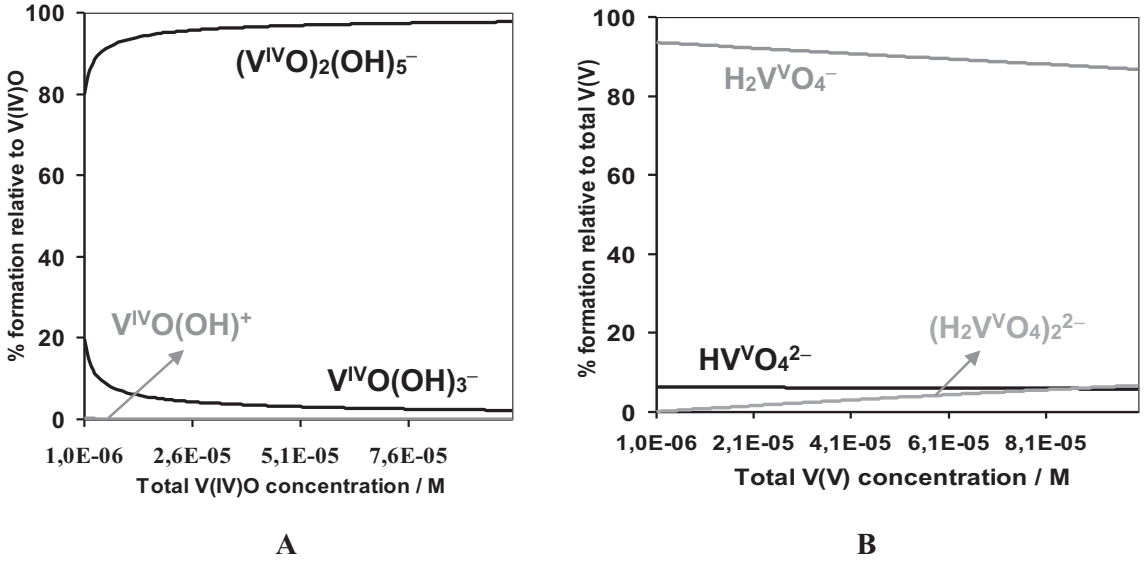

Fig. 1. Concentration distribution diagram for the hydrolysis of (A) oxidovanadium(IV) and (B) dioxidovanadium(V) at pH = 7.0, calculated using the HySS computer program [30], in the concentration range (total) of V^{IV} and V^{V} between 1×10^{-6} and 1×10^{-4} M. The stability constants values for V^{IV} correspond to Eq. 1 and for V^{V} to Eq. 2.

between 5 and 13 min. Notwithstanding, the + IV state can be significantly stabilized when a suitable organic ligand is present, or a bioligand (such as a protein), this probably extending significantly the lifetime of $V^{IV}O$-species.

Vanadate(V) can be present in several chemical forms, oligomeric or monomeric, this depending on the pH, ionic strength and total vanadium concentration [21] [26] [27] [28]. If V^{IV} is present the species that predominate also depend on pH and total vanadium concentration [21] [29]. Fig. 1 depicts concentration distribution diagrams for the hydrolysis of $V^{IV}O^{2+}$ and $V^{V}O_2^{+}$, calculated using the HySS computer program [30], in the concentration range of V^{IV} and V^{V} between 1×10^{-6} and 1×10^{-4} M (total concentrations), the range expected to be relevant in most biological systems, as well as in most electrochemical experiments. For the oxidovanadium(IV) system the stability constants are defined according to Eq. 1 [21] [29], and for the dioxidovanadium(V) system (or vanadate(V) system) they are defined here based on $H_2V^{V}O_4^{-}$ according to Eq. 2 [26].

$$p\ V^{IV}O^{2+} + r\ H^{+} \leftrightarrows (V^{IV}O)_p(H)_r \quad (1)$$

$$p\ H_2V^{V}O_4^{-} + r\ H^{+} \leftrightarrows (H_2V^{V}O_4)_p(H)_r \quad (2)$$

Because apo-hTF does not absorb visible radiation and as vanadium (V) has no d-electrons, in solutions containing vanadate(V) and apo-hTF at pH 7.4 no electronic bands show up for $\lambda > 400$ nm; only bands due to e.g. charge-transfer transitions may be recorded if intense enough. Upon additions of a $NaV^{V}O_3$ solution to hTF the circular dichroism (CD) spectra in the 200–350 nm range show significant changes [31]. Although it is not clear why these changes occur, they are the result of interaction of V^{V}-species with chiral centers of apo-hTF. The bands at ca. 300–350 nm are probably due to phenolate-O^{-} to V^{V} charge transfer transitions. Harris [32] proposed the binding of V^{V} close to the iron hTF binding sites. It was also reported that apo-hTF is able to bind two equivalents of V^{V} in the presence or absence of the synergistic carbonate anion, which is necessary for the coordination of other metal ions [8], but not for V^{V} ions.

Several distinct techniques have been used to study the interaction of V^{V} with apo-hTF [8] (and refs therein) [25] [33] [34], and conditional binding constants (K′) have been reported. The constants obtained from calorimetric [34] and ultrafiltration [35] data are at least one order of magnitude lower than those derived from difference UV measurements [33]. More recently, from ^{51}V NMR spectroscopy Jakusch et al. [8] determined log (K'_1) = 6.0 and log ($K'_1K'_2$) = 11.5 for (V^{V})(apo-hTF) and (V^{V})$_2$(apo-hTF), respectively, these being consistent with data from ultrafiltration experiments. The binding constants K'_1 and K'_2 correspond to conditional stability constants, valid in the experimental conditions of the medium used (in the above cases at pH = 7.4), defined according to Eq. 3:

$$K'_p.\ :apo - hTF + pV^{V} \leftrightarrows [(V^{V})_p(apo - hTF)] \quad (3)$$

In the ^{51}V NMR spectra of solutions of vanadate(V) and apo-hTF at pH ~7.4 two distinct ^{51}V NMR chemical shifts are detected at $\delta_V = -529$ and -531 ppm (shoulder, often not clearly visible), and these were assigned to binding at residues of the C- and N-terminal sites [36]. In a previous study [31] some of us discussed several aspects concerning the probable relevance of binding of V^{V} to apo-hTF and holo-hTF; the binding of $V^{IV}O^{2+}$ to holo-hTF has also been addressed [37]. It is possible that a small amount of vanadate may act as a synergistic anion or bind close to the Fe-binding site; it was suggested that besides the possibility of uptake of vanadate by cells through phosphate channels, its uptake through holo-hTF endocytosis cannot be ruled out.

It was also confirmed that V^{III} binds strongly to apo-hTF [10] [31] [38] [39] and that (V^{III})$_2$(apo-hTF) corresponds to a 'closed conformation' similarly to holo-hTF [31]. The possibility of formation of V^{III}-species in blood has been proposed by several other authors [15] [40] [41]; whether (V^{III})$_2$hTF or (Fe^{III}/V^{III})hTF complexes [31] may form or not in blood serum, thus having the possibility of being uptaken by receptor-mediated endocytosis, is a subject that needs and deserves further research to be fully clarified.

Based on EPR measurements made immediately after the preparation of the solutions at pH 7.4, in the absence of dioxygen it was proposed that $V^{IV}O$-species may bind to holo-hTF [37], but it is not clear how fast these $V^{IV}O$-species may oxidize in blood serum conditions. By UV difference spectroscopic experiments Harris and Carrano [33] obtained evidence for the binding of a small amount of V^{V} to holo-hTF (up to ca. 2:0.14 (Fe:V molar ratio)) and analyzing the V and Fe content in desalted samples containing holo-hTF and vanadate(V) at pH 7.4 by ICP-AES, it was shown that V^{V} binds to holo-hTF (ca. 2:0.29 (Fe:V molar ratio)) [31]. The binding of V^{V} to holo-hTF may thus be relevant for the up-take of vanadium by cells and in this work we evaluate the binding by electrochemical techniques, matrix-assisted laser desorption/ionization time of flight (MALDI-TOF) mass spectrometry and small-angle X-ray scattering (SAXS).

Voltammetric methods have been widely used to investigate metal ion complexation taking advantage of the electro activity of the metal

ions and/or the complexes formed, and less frequently of the ligands. Vanadium has a rich and diverse redox chemistry due to the variety of easily accessible oxidation states and early studies of its oxidation/reduction chemistry in aqueous solution were reported by Lingane [42]. The behavior of all oxidation states in non-complexing media and in the presence of small ligands was investigated by classic polarography in different electrolytes [43]. More recently the vanadium electrochemistry and of its complexes were the subject of two reviews [44] [45]. Most reports dealt with the complexation by small molecules, no studies being found concerning the electrochemistry of vanadium-protein complexes.

As to the human serum transferrins, the voltammetric behavior of holo-hTF and apo-hTF solutions at silver electrode was the subject of one publication. The experiments were done at pH = 7.2 and a voltammetric signal at − 0.42 V vs saturated calomel electrode (SCE) was observed and attributed to an irreversible reduction of holo-hTF adsorbed on the electrode surface; the protein in the apo-form was non-electroactive [46]. Lack of electrochemical response from solutions containing apo-hTF was also observed at modified glassy carbon electrode [47].

To the best of our knowledge electrochemical methods have not been used to study the interactions between vanadium and the human serum transferrins. In this work we report the use of two different voltammetric techniques: Differential Pulse Polarography (DPP) and Cyclic Voltammetry (CV), with different time windows, to investigate the electrochemical behavior of vanadium in the presence of holo-hTF and apo-hTF. The experiments carried out herein intend to evaluate the affinity and binding of vanadium(V) to human serum transferrins and their effects on the redox behavior in aqueous solution of V^{V}, V^{IV}, V^{III} and V^{II} species.

To be close to the pH of physiological media, all experiments were done at pH 7.0 ± 0.1. At this pH the main V^{IV}- or V^{V}-species present are shown in Fig. 1. For the $V^{IV}O^{2+}$ system the main hydrolytic species present in the experimental conditions of the electrochemical experiments are $\{(V^{IV}O)_2(OH)_5^-\}_n$ and $V^{IV}O(OH)_3^-$ (the value of n depends on the total V^{IV} concentration) [21] [29], and for the vanadate system the main hydrolytic species present are $H_2VO_4^-$, HVO_4^{2-} (both sometimes designated by V_1) and $H_4V_2O_8$ (one of the dinuclear species of vanadate(V), these sometimes designated by V_2) [26].

MALDI-TOF mass spectrometric and SAXS experiments were also carried out to confirm the binding of V^{IV} and V^{V} species to hTF.

2. Materials and methods

2.1. Chemicals and solutions

All solutions were prepared from analytical grade reagents, except otherwise stated, using distilled or deionised water from a Milli-Q 185 Plus water purification system (Millipore, Bedford, MA, USA). The vanadium(V) stock solutions (10 mM) were prepared by dissolution of $NaV^{V}O_3$ in a NaOH solution adjusted to pH 10.4 ± 0.1 The solution was allowed to boil for 10 min, cooled to room temperature and the pH readjusted with NaOH solution. This procedure was repeated twice to ensure the absence of any decavanadates (V_{10} species). The stock solutions were kept under refrigeration (at ca. 5 °C).

The apo-hTF (Prospec) and holo-hTF (Sigma, T4132) stock solutions were prepared by dissolving the solid protein (ca. 50 mg) in the supporting electrolyte/buffer (0.5 mL) in order to obtain solutions with ca. 1 mM concentration (or less). The hTF concentrations were checked by measuring their extinction coefficients at 280 nm: apo-hTF ($\varepsilon = 9.23 \times 10^4\ M^{-1}\ cm^{-1}$) [25] and holo-hTF ($\varepsilon = 1.13 \times 10^5\ M^{-1}\ cm^{-1}$) [48].

Voltammetric analyses were done in the supporting electrolyte/buffer: $NaHCO_3$ (0.01 M), NaCl (0.1 M) and HEPES (0.1 M), adjusted to pH = 7.0 ± 0.1 by the addition of HCl (1 M). Hereafter we will designate this solution by “buffer”; most of the results reported correspond to experiments carried out with pH = 6.95 (pH value measured).

2.2. Instrumentation and procedures

2.2.1. Electrochemical experiments

The voltammetric measurements were carried out using a potentiostat/galvanostat from ECO Chemie, Autolab PSTAT12 (Utrecht, The Netherlands) as the source of the applied potential and as the measuring device, connected to the Metrohm Stand 663 (Herisau, Switzerland) featuring a conventional three-electrode configuration: a Static Mercury Drop Electrode (SMDE) as the working electrode, an $Ag/AgCl/KCl_{(sat)}$ as the reference electrode and a carbon rod auxiliary electrode. The whole system was controlled and data analyzed with the GPES software (General Purpose Electrochemical System version 4.9) from ECO Chemie B.V. (Utrecht, The Netherlands). pH measurements were carried out using a Crison GLP 21 digital pH meter coupled with an InLab Micro pH electrode (Mettler Toledo).

Differential pulse polarography (DPP) and cyclic voltammetry (CV) were used to analyze the binding of vanadium to human apo-transferrin and to human holo-transferrin. In DPP, the initial potential, E_i, was 0.1 V and the final potential, E_f, was − 1.25 V, a differential pulse amplitude, $E_{DP,}$ of |50| mV, a step height, $E_{SH,}$ of 5 mV, a pulse amplitude, t_p, of 0.05 s and a repetition period (drop time) of 0.5 s were used.

In most experiments, the total vanadium(V) concentration, $[V^{V}]_{total}$, was 9.73×10^{-5} M; the total holo-hTF concentrations, $[holo\text{-}hTF]_{total}$, were varied between 0 and $\sim 1.8 \times 10^{-4}$ M, and the total apo-hTF concentrations, $[apo\text{-}hTF]_{total}$, between 0 and $\sim 7.1 \times 10^{-5}$ M. The handling and addition of the vanadate stock solutions were always done never allowing, even for short periods of time, the V^{V}-containing solutions to have pH values lower than ~6.9.

The voltammetric response of vanadium was calibrated in the absence of the proteins, in the same electrolyte medium.

In CV, E_i was set equal to E_f and equal to 0.1 V and in most experiments the direction of the scan was reversed at $E_\lambda = -1.20$ V. The scan rate (v) varied between 10×10^{-2} and 0.2 V/s. Similar total concentrations of vanadium and proteins were used as in the DPP experiments.

Adsorption of the proteins on the mercury electrode surface was studied by alternating current voltammetry (ACV). The measurements were done with apo-hTF and holo-hTF solutions in the supporting electrolyte and in the absence of vanadium. An alternating potential of 5 mV with a frequency of 66 Hz was superimposed on a linear voltage ramp that varied between 0.1 V and − 1.25 V. The alternating component of the current was recorded in that potential range at a phase angle of 90°.

Throughout this work potential (E) values are referred to a saturated silver/silver chloride electrode (205 mV vs. standard hydrogen electrode) and are affected by an error of ± 5 mV. Before each voltammetric measurement the solutions were purged with N_2 during ~15 min and a continuous flow was kept on the top of the solutions during all experiments. All measurements were done at least in duplicate and in a room with temperature controlled at 25 ± 1 °C.

2.2.2. MALDI-TOF mass spectrometric experiments

Mass spectra were obtained using a Bruker Daltonics Ultraflex MALDI TOF/TOF Mass Spectrometer operating in linear mode with positive ion extracting at 25,000 V and a pulsed ion extraction of 480 ns. Each final spectrum was the accumulated result of at least 1000 laser shots that were obtained from 10 different manually selected regions of the same sample, over a range of 14,000–100,000 Da. Prior to calibration, the spectra were processed with Compass 1.3 using smoothing and baseline subtraction for reproducible peak annotation. The spectra were externally calibrated using of 50 pmol of bovine serum albumin ($[M + H]^+$ 66,430).

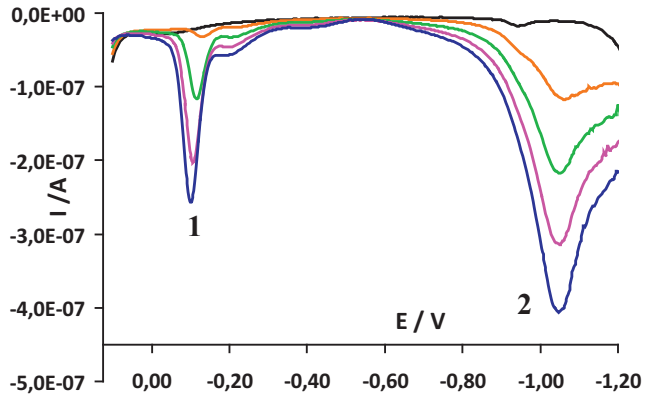

Fig. 2. Differential pulse polarograms of solutions containing vanadium (V) at different $[V^V]_{total}$ concentrations (M): black, 0; orange, 2.46×10^{-5}; green, 4.91×10^{-5}; violet, 7.35×10^{-5}; blue, 9.85×10^{-5}. Voltammetric conditions: $E_i = 0.1$ V; $E_f = -1.25$ V; $E_{DP} = 50$ mV; $E_{SH} = 5$ mV; $t_p = 50$ ms. Medium: "buffer" (pH 6.95) and t = (25 ± 1) °C. Peak 1: $V^V \rightarrow V^{IV}$ reduction, peak 2: $V^{IV} \rightarrow V^{II}$ reduction. (For interpretation of the references to colour in this figure legend, the reader is referred to the web version of this article.)

2.2.2.1. Sample preparation. The $NH_4V^VO_3$ stock solutions ca. 3 mM were prepared as described above. The $V^{IV}OSO_4$ was prepared immediately before the experiments. Solutions of apo-hTF and holo-hTF were prepared with ca. 300 μM concentration, by dissolving the protein in NH_4HCO_3 buffer (pH 7.4, 25 mM). These solutions were allowed to stand overnight to allow equilibration. Their concentrations were determined by measurement of the UV absorption at 280 nm.

Samples for MALDI-TOF mass spectrometric experiments were prepared with $V^{IV}OSO_4$:apo-hTF, $NH_4V^VO_3$:apo-hTF and $NH_4V^VO_3$:holo-hTF molar ratios of 0:1 and 3:1 (also 5:1 for $V^{IV}OSO_4$:apo-hTF samples) by mixing different volumes of the stock solutions with buffer. The transferrin concentrations were ~50 μM.

2.2.2.2. Dried Droplet preparation. 2 μL of each sample were mixed with 2 μL of matrix solution (saturated solution of sinapinic acid in 1 mL of 30% (v/v) acetonitrile and 0.1% (v/v) aqueous trifluoroacetic acid). Then 1 μL of the sample-matrix solution was deposited by duplicate onto a MTP 384 ground steel BC target and allowed to dry at room temperature. The apo-hTF and holo-hTF concentrations of the final samples were thus 25 μM.

Several analyses were made, as described above, for each sample prepared. The masses somewhat varied and average values were obtained for the masses for each set of samples (of apo-hTF, holo-hTF, $V^{IV}OSO_4$ + apoHTF, $NH_4V^VO_3$ + apo-hTF and $NH_4V^VO_3$ + holo-hTF).

2.2.3. Small-angle X-ray scattering (SAXS) experiments

2.2.3.1. Sample preparation. A first sample of apo-hTF (15 mg/mL, 500 μL in 20 mM Tris-HCl pH 8, 20 mM sodium carbonate and 200 mM sodium chloride) was prepared. A second sample of apo-hTF (15 mg/mL, 500 μL in similar buffer) was incubated for one hour at room temperature with a 10 times molar equivalent excess of $V^{IV}OSO_4$. A third sample of apo-hTF (8 mg/mL, 500 μL in similar buffer) was incubated for one hour at room temperature) with a 10 times molar equivalent excess of NaV^VO_3. Immediately prior to data collection, the samples were passed through PD-10 MiniTrap G-25 columns (dilution to 7.5 and 4 mg/mL, respectively) in order to assure a proper buffer match as well as to remove unbound metal ions.

Similar experiments were carried out with human serum holo-transferrin (holo-hTF) and three samples: holo-hTF, holo-hTF - $V^{IV}OSO_4$ and holo-hTF - NaV^VO_3 were obtained for this purpose.

2.2.3.2. Data collection and processing. The six prepared samples were analyzed by SAXS and the data was collected at beamline BM29 (ESRF, Grenoble, France) [49] [50]. Different concentrations ranges were prepared according to the sample: 7.5 to 0.47 mg/mL (apo-hTF and holo-hTF), 7.5 to 0.23 mg/mL (apo-hTF + $V^{IV}OSO_4$ and holo-hTF + $V^{IV}OSO_4$) and 4 to 0.5 mg/mL (apo-hTF + NaV^VO_3 and holo-hTF + NaV^VO_3). For each concentration, ten frames of one second each were collected at 25 °C.

Data were reduced and analyzed using Scatter (Diamond Light Source, UK) and the ATSAS suite [51]. Each experimental frame was inspected for radiation damage and those affected were not used for buffer subtraction. Theoretical SAXS curves were calculated using CRYSOL [52]. The dimensionless Kratky plot and the P(r) function (pair distance distribution function) were performed in Scatter. Systems which are plotted with a dimensionless Kratky plot have peak at square root 3 (x-axis) with magnitude of $3e^{-1}$ (i.e. 1.1036) if the system obeys Guinier's law and is globular [53]. An ensemble of seven low resolution envelope models were generated from the P(r) function in DAMMIF and then subject to averaging and filtering with DAMAVER and DAMFILT [54] [55]. The output from DAMFILT was then passed to DAMMIN as a start model for final refinement against the experimental curve [56].

3. Results and discussion

3.1. Differential pulse polarography

3.1.1. Behavior of V^V in the absence of the proteins

Fig. 2 depicts the DP polarograms of vanadium solutions in the "buffer" at pH = 6.95 while varying the V^V concentration in the range (2.5–9.8) $\times 10^{-5}$ M. Two reduction peaks, peak 1 and peak 2, are detected at peak potentials $E_p^1 = -0.110$ V and $E_p^2 = -1.045$ V.

As to the number of electrons (n) exchanged in the two redox processes, the assignment of n cannot be simply done from peak widths at half height ($W_{1/2}$), as diagnostic criteria based on peak current and peak potential variations with the sign of differential pulse amplitude, E_{DP} [57], showed that the reactions are not reversible. The same is true from peak current analysis since the degree of non-reversibility may affect differently both peak currents. Additionally the shape of peak 1, namely $W_{1/2} \approx 0.050$ V, suggests the occurrence of adsorption [58]. Both i_p^1 and i_p^2 vary linearly with the $[V^V]_{total}$ concentrations, with $r > 0.99$ and a null intercept but identical slopes, as can be seen in Fig. SI-1-1. This behavior puts forward that peak 1 is under the influence of adsorption phenomena, most probably of both reactant and product [59], through the adsorption of the negatively charged species of V^V and V^{IV}. At pH 7 and total vanadium concentrations of 9.73×10^{-5} M the hydrolytic V^V and V^{IV} species expected to be present are indeed anionic (see Fig. 1).

The number of electrons exchanged may be estimated from peak area analysis [58]. Both peak areas, A_p^1 and A_p^2, vary linearly with $[V^V]_{total}$ with $r > 0.98$ and a null intercept, and slopes that differ by a factor of two (see Fig. SI-1-2). This means that the number of electrons associated to peak 2 is twice the number of electrons involved in peak 1. Therefore the first reduction wave (peak 1) can be assigned to the one electron reduction of V^V to V^{IV} ions according to schematic reaction 4:

$$V^V + 1e^- \rightarrow V^{IV} \quad (4)$$

While the second wave (peak 2) is due to the two electron reduction of V^{IV} to V^{II} ions, according to the schematic reaction 5:

$$V^{IV} + 2e^- \rightarrow V^{II} \quad (5)$$

This is in agreement with the reported behavior using classic polarography of solutions containing vanadium(V) in diluted acid media where V^V undergoes stepwise reduction to the V^{IV} and V^{II} states. Although the reaction $V^{III} \rightarrow V^{II}$ is a reversible process at a mercury electrode, the same does not happen with the reaction $V^{IV} \rightarrow V^{III}$, which is an irreversible process and so the redox reaction proceeds directly from $V^{IV} \rightarrow V^{II}$ [43]. Since at pH = 7.0 and total vanadium concentrations used in this study the main V^V species is $H_2V^VO_4^-$ and the

main V^{IV} species is $\{(V^{V}O)_2(OH)_5{}^-\}_n$ (n depends on the total V concentration), reactions (4) and (5) are pH dependent.

Several attempts to differentiate the stepwise reduction of $V^{IV} \rightarrow V^{III}$ and $V^{III} \rightarrow V^{II}$ species, using DP voltammetry (DPV) at different electrodes were unsuccessful. Carbon electrodes (glassy carbon, modified glassy with lipid layer cationic-type, modified electrode with carbon nanotubes), pyrolitic graphite (in presence or absence of such promoters as neomicine, poly-L-lysine, didodecyldimethylammonium bromide, DDAB), gold electrode (in presence or absence of neomicine), platinum electrode and ultra-trace graphite were tested. Only the reduction $V^{IV} \rightarrow V^{II}$ was barely seen at a ultragraphite electrode when $[V^{V}]_{total}$ concentrations higher than 6×10^{-4} M were used. Our results are in conformity with the lack of electrochemical response of the V^{V} state at other electrodes than at the mercury electrode.

3.1.2. Behavior of solutions containing vanadate(V) in the presence of the proteins

No signals were detected in the differential pulse polarograms of solutions containing only apo-hTF in the supporting electrolyte at pH = 7.0 ± 0.1, showing that the apo-hTF is non-electroactive, in the studied potential range, at a mercury electrode. These results are in agreement with the absence of electrochemical response from solutions containing apo-hTF at modified glassy carbon electrode [47] and at silver electrode [46]. Upon adding apo-hTF to solutions containing vanadium(V) so that $[V^{V}]_{total} = 9.85 \times 10^{-5}$ M and $[\text{apo-hTF}]_{total} = (3.6–7.1) \times 10^{-5}$ M, peak 1 and peak 2 retain the same non-reversible characteristics as in the medium not containing the protein, as far as could be evaluated using again negative ongoing potential pulses, followed by positive potential pulses [57]. However, both peak currents are affected (Fig. 3). Regarding peak 2, its potential remains the same within experimental error, as well as its shape. As to peak 1, there is a small cathodic shift after protein addition and it loses its sharpness, with $W_{1/2} = 0.110$ V in the presence of protein and 0.050 V in the absence of the protein. Most importantly, for both peaks the current decreases with increasing apo-hTF concentration in solution (Fig. 3).

Unlike spectroscopy techniques, electroanalytical techniques are not suitable to provide information about structure. Nevertheless, depending on medium conditions, changes in the relationship between potential and current might occur as a consequence of the interactions in solution between the electroactive species and other molecules, namely due to complexation. The behavior described clearly demonstrates that apo-hTF binds to vanadium both in the V^{V} and V^{IV} states. The complexes formed are inert in terms of the time scale of the technique used, i.e. dissociation does not occur during the reduction and

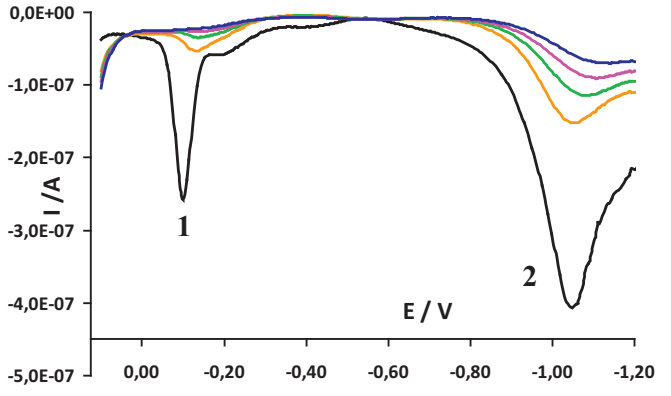

Fig. 3. Differential pulse polarograms of solutions containing vanadate(V) with $[V^{V}]_{total} = 9.85 \times 10^{-5}$ M, in the absence (black line) and upon additions of apo-hTF, $[\text{apo-hTF}]_{total}$ (M): orange, 3.60×10^{-5}; green, 4.80×10^{-5}; violet, 6.00×10^{-5} and blue 7.08×10^{-5} Voltammetric conditions: $E_i = 0.10$ V; $E_f = -1.20$ V; $E_{DP} = 50$ mV; $E_{SH} = 5$ mV; $t_p = 50$ ms. Medium: "buffer", pH 6.95 and t = (25 ± 1) °C. Peak 1: $V^{V} \rightarrow V^{IV}$ reduction, peak 2: $V^{IV} \rightarrow V^{II}$ reduction. (For interpretation of the references to colour in this figure legend, the reader is referred to the web version of this article.)

therefore the peak areas of the voltammetric signals are directly related to the vanadium in solution not bound to the protein [60]. The V-protein complexes formed are also non-electroactive over the potential range studied since no further peaks were detected.

Assuming that vanadium binds to the macromolecule forming a complex [20] [25] [31] [35] [36] [61], then the interaction between the metal ion and the protein can be described by Eq. 3, and the conditional stability constants K'_p are given by Eq. 6:

$$K' = [(V^{V})_p(\text{apo} - \text{hTF})]/[V^{V}]^p[\text{apo} - \text{hTF}] \quad (6)$$

where $[(V^{V})_p(\text{apo-hTF})]$ is the concentration of complex, [apo-hTF] is the protein concentration not bound to vanadium, $[V^{V}]$ is the total vanadate concentration not bound to apo-transferrin (mostly V_1: $H_2VO_4{}^-$ and $H_2VO_4{}^{2-}$, but also V_2, see e.g. Fig. 1B) and p represents the number of V^{V} ions bound to the protein. K'_p may be computed from the mass balance equations for the metal ion and the protein, Eqs. 7 and 8, respectively.

$$[V^{V}]_{total} = p\,[(V^{V})_p(\text{apo} - \text{hTF})] + [V^{V}] \quad (7)$$

$$[\text{apo} - \text{hTF}]_{total} = [(V^{V})_p(\text{apo} - \text{hTF})] + [\text{apo} - \text{hTF}] \quad (8)$$

where $[V^{V}]$ is directly determined from the DP polarograms' peak areas through the calibration plot. Calculations were done using either the areas of peak 1 or peak 2 and assuming the formation of $[(V)_p(\text{apo-hTF})]$ with stoichiometry 1:1 or 2:1, or a mixture of 1:1 and 2:1 complexes. The treatment of the experimental data as described showed that in our experimental conditions only one complex predominates in solution, $[(V^{V})_2(\text{apo-hTF})]$. The individual values computed for K'_p presented in Table 1 also show that similar results were obtained using either peak 1 due to $V^{V} \rightarrow V^{IV}$ reduction or peak 2 due to $V^{IV} \rightarrow V^{II}$ reduction. This means that the reduction of V^{V} to V^{IV} does not decompose the V-protein complexes initially formed. Consequently an average conditional stability constant of $\log K'_{(V)2(\text{apo-hTF})} = 10.2 \pm 0.4$ was calculated.

The value here obtained for $\log K'_{(V)2(\text{apo-hTF})}$ is reasonably similar to those determined by Kiss and co-workers (= 11.5) [8] and Harris and Carrano [33] (~11.5) at distinct ionic media and pH (pH = 7.4), while Bordbar et al. [34] only assumed the formation of $(V^{V})_1$(apo-hTF) with $K' \sim 10^5$.

Regarding the voltammetry of holo-hTF, in the experimental conditions used no signals were found from solutions containing only the protein in the electrolyte. When holo-hTF is added to a solution containing vanadate(V), so that $[V^{V}]_{total} = 9.85 \times 10^{-5}$ M and $[\text{holo-hTF}]_{total} = (2.4–12.6) \times 10^{-5}$ M, a similar behavior is observed as described before in the presence of apo-hTF. Peaks 1 and 2 remain with the same non-reversible nature as in the non-complexing medium. Peak potentials stay the same, as well as the shape of the polarogram in the case of peak 2. For peak 1 the DP polarogram is no longer sharp, and there is a small cathodic shift after protein additions, as can be seen in Fig. 4. With the increase of holo-hTF concentration in solution, peak intensities also decrease as observed for apo-hTF, though less pronounced for similar protein concentrations, this probably reflecting distinct binding. In spite of the different binding sites of vanadium to the proteins [7] [37] this behavior clearly demonstrates that holo-hTF also binds vanadium, the complexes formed being inert and non-electroactive (at the mercury electrode).

Table 1
Conditional stability constants (log K′) of $[(V^{V})_2(\text{apo-hTF})]$ complexes in $NaHCO_3$ (0.01 M), NaCl (0.1 M) and HEPES (0.1 M), pH = 6.95 and t = (25 ± 1) °C.

$[V^{V}]_{total}$/M	$[\text{apo-hTF}]_{total}$/M	log K′$_2$(peak 1)	logK′$_2$(peak 2)
9.60×10^{-5}	3.60×10^{-5}	9.8	9.6
9.55×10^{-5}	4.77×10^{-5}	10.5	10.5
9.49×10^{-5}	5.93×10^{-5}	10.4	10.5
9.43×10^{-5}	7.08×10^{-5}	10.2	10.3

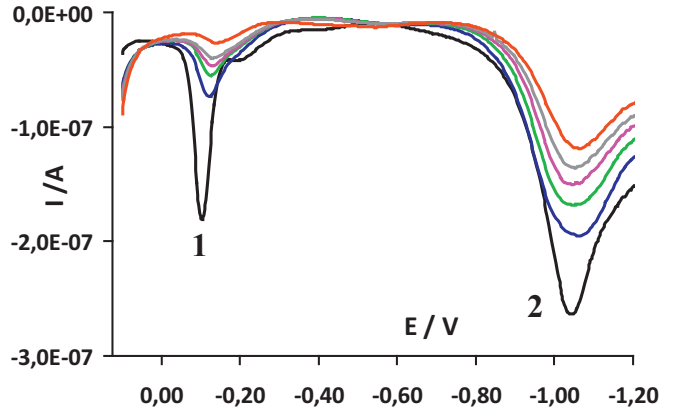

Fig. 4. Differential pulse polarograms of solutions containing vanadate(V) with $[V^V]_{total} = 9.85 \times 10^{-5}$ M, in the absence (black line) and upon addition of holo-hTF, $[holo\text{-}hTF]_{total}$ (M): blue, 2.42×10^{-5}; green, 4.77×10^{-5}; pink, 7.08×10^{-5}; grey, 9.32×10^{-5} and red, 12.6×10^{-5}. Voltammetric conditions: $E_i = 0.1$ V; $E_f = -1.25$ V V; $E_{DP} = 50$ mV; $E_{SH} = 5$ mV; $t_p = 50$ ms. Medium: "buffer" (pH 6.95) and t = (25 ± 1) °C. Peak 1: $V^V \rightarrow V^{IV}$ reduction, peak 2: $V^{IV} \rightarrow V^{II}$ reduction. (For interpretation of the references to colour in this figure legend, the reader is referred to the web version of this article.)

As described previously for the protein in the apo-form, calculations were done using the total mass balances for the metal ion and the protein (Eqs. 7 and 8), the areas of peak 1 or peak 2 and assuming the formation of 1:1 or 2:1 or a mixture of 1:1 and 2:1 complexes. For our experimental conditions the voltammetric data could be explained by the formation of 1:1 and 2:1 complexes with average conditional stability constants $\log K'_{(V)1(holo\text{-}hTF)} = 4.3 \pm 0.5$ and $\log K'_{(V)2(holo\text{-}hTF)} = 8.3 \pm 0.6$.

For both systems additional sets of experiments were done adding the stock solution of V^V to protein solutions in the supporting electrolyte. Due to adsorption of the proteins as non-electroactive species on the electrode surface, the voltammetric data were less reproducible; experiments were done for $[V^V]_{total}$:$[apo\text{-}hTF]_{total} = 2$ and $[V^V]_{total}$:$[holo\text{-}hTF]_{total} = 2$ and 1. The behavior observed is also consistent with the binding of vanadium to the proteins, the hTF-V complexes formed being electrochemically inert. The conditional stability constants estimated for the 2:1 complex of V^V with apo-hTF is $\log K'_{(V)2(apo\text{-}hTF)} = 11 \pm 1$ and for the 1:1 and 2:1 complexes of V^V with holo-hTF are: $\log K'_{(V)1(holo\text{-}hTF)} = 4.3 \pm 0.7$ and $\log K'_{(V)2(holo\text{-}hTF)} = 8.8 \pm 0.8$, being in reasonable agreement with the values mentioned above.

The voltammetric behavior here observed for the apo-hTF-V^V and holo-hTF-V^V complexes agrees with reported electrochemical studies (differential pulse stripping voltammetry) on the binding of lead ions to serum proteins, namely bovine apo-TF [47]. The peak current due to lead reduction at a modified glassy carbon electrode decreased in the presence of the protein, while peak potentials remained constant indicating the formation of electrochemically inert complexes between Pb^{2+} and bovine apo-TF. A log $K'_1 = 4.0$ was determined for the 1: 1 complexes in acetate buffer 0.2 M at pH = 5 [47].

3.2. Cyclic voltammetry

3.2.1. Behavior of V^V in the absence of the proteins

Fig. 5 shows cyclic voltammograms of solutions containing vanadate(V), measured at different scan rates. Two reduction peaks, 1 and 2, are observed in the potential range between 0.1 V and −1.20 V for scan rates between 0.010–0.200 V/s. Furthermore, an oxidation peak, peak 3, is observed in the reverse scan. The reduction peaks 1 and 2 are not reversible, as can be concluded by the reduction peak potentials which shift to more negative potentials with increasing scan rates (this more clearly seen for peak 1). For comparison purposes with the DP data, for scan rates 0.010 V/s and 0.100 V/s, the data is: $E_{pc}{}^1 = -0.110$ V, $E_{pc}{}^2 = -1.000$ V and $E_{pc}{}^1 = -0.120$ V, $E_{pc}{}^2 = -1.035$ V, respectively. Taking into account these potentials and the previous discussion of the differential pulse data, the two reduction peaks correspond to the stepwise reductions: $V^V \rightarrow V^{IV}$ and $V^{IV} \rightarrow V^{II}$.

The degree of non-reversibility differs between the two reactions, as easily seen on the CVs. The redox reaction responsible for peak 2 is irreversible, since no anodic peak is observed on the reverse scan. The first redox reaction (the $V^V \rightarrow V^{IV}$ process), can be considered quasi-reversible, peak 3 being the anodic counterpart of peak 1 (the oxidation $V^{IV} \rightarrow V^V$) with potentials $E_{pa}{}^3$ (for scan rate 0.010 V/s, $\Delta Ep = E_{pa}{}^3 - E_{pc}{}^1 = 0.135$ V). These results are also in agreement with the previously described classic polarographic behavior of V^V and its stepwise reduction to the V^{II} state [43]. No other signals were identified that could be attributed to a stepwise process involving the V^{III} state.

Peaks 1 and 3 are under the influence of adsorption of both reactant and product, this being more clearly seen in the anodic peak [62]. Comparing the CV of the supporting electrolyte with that obtained upon adding the V^V-containing solution (Fig. 6) it is clear that adsorption is due to negatively charged species of V^V and V^{IV}, as expected from the speciation (Fig. 1).

The shape of the peaks as well as the variation of the peak currents, $i_{pc}{}^1$ and $i_{pa}{}^3$, with the scan rate confirms the existence of adsorption of the electroactive species. Both vary linearly with v although with a different intercept as can be seen in Fig. SI-1-3. This is what can be expected for an adsorption controlled quasi-reversible process with different transfer coefficient, α, for the reduction and oxidation reactions [58]. In summary, the quasi-reversible redox reaction $V^V \rightarrow V^{IV}$ occurs under the influence of both reactant and product adsorption (peaks 1 and 3). Peak 2 is not under the influence of any adsorption since $i_{pc}{}^2$ varies linearly with the square root of v with $r > 0.995$ and a null intercept (Fig. SI-1-3). Therefore peak 2 corresponds to the diffusion controlled irreversible reaction of $V^{IV} \rightarrow V^{II}$.

To further clarify the surface processes several other scans were done. The direction of the scan rate, either with $E_i = E_f = 0.10$ V and $E_\lambda = -1.20$ V, or $E_i = E_f = -1.20$ V and $E_\lambda = 0.10$ V, does not affect, within the experimental error, the reduction peaks 1 and 2, as can be concluded by the voltammograms depicted in Fig. 7. The direction of the scan has a pronounced effect on peak 3, as may be seen in Fig. 7. Adsorption effects were already present on the DPP data, but are more pronounced in the CV, since a stationary electrode is used and more time is available for adsorption on the electrode surface; when the potential is scanned in the range 0.10 V to −0.30 V, the anodic peak $E_{pa}{}^3$ is much less affected, as can also be seen in Fig. 7. The cyclic voltammogram in the range −0.90 V to −1.20 V shows an irreversible cathodic wave due to $V^{IV} \rightarrow V^{II}$ reduction, whose intensity is not affected, but interestingly a small cathodic shift is observed on the potential, most certainly due to changes in the electrode surface due to the different adsorption effects in this range of potentials.

3.2.2. Behavior of V^V in the presence of the proteins

Fig. 8 depicts the CVs voltammograms at v = 80 mV/s for reduction of V^V in the absence (peaks 1, 2 and 3) and in presence of apo-hTF (peaks 2′ and 3′). Similar CV voltammograms for reduction of V^V were obtained with holo-hTF (data not shown).

Several aspects should now be considered. Peak intensities decrease with the increase of protein concentration. Due to differences in sensitivity between DPP and CV, the reduction peak at potentials close to peak 1 is hardly seen, though its anodic counterpart, peak 3′, is still detected for the lowest protein concentrations. A second irreversible signal, peak 2′, at potentials related to peak 2 is also observed. No other voltammetric signals were detected for all scan rates in the potential range under study. The peak potential of peak 2 shifts cathodically after the first addition of the proteins and then remains constant, within the experimental error. Moreover, the CVs become quite flat after protein addition, i.e., the capacitive current changed markedly in the presence

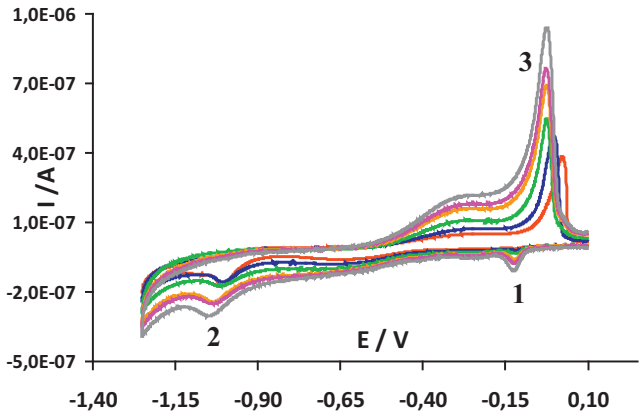

Fig. 5. Cyclic voltammograms of solutions containing vanadate(V) with $[V^V]_{total} = 9.85 \times 10^{-5}$ M and different scan rates (mV/s): red, 0.010; blue, 0.020; green, 0.040; orange, 0.080; violet, 0.100 and grey, 0.150. Other voltammetric conditions: $E_i = E_f = 0.10$ V $E_\lambda = -1.20$ V. Medium: "buffer" (pH 6.95) and t = (25 ± 1) °C. Peak 1: $V^V \rightarrow V^{IV}$ reduction, peak 2: $V^{IV} \rightarrow V^{II}$ reduction, peak 3: $V^{IV} \rightarrow V^V$ oxidation. (For interpretation of the references to colour in this figure legend, the reader is referred to the web version of this article.)

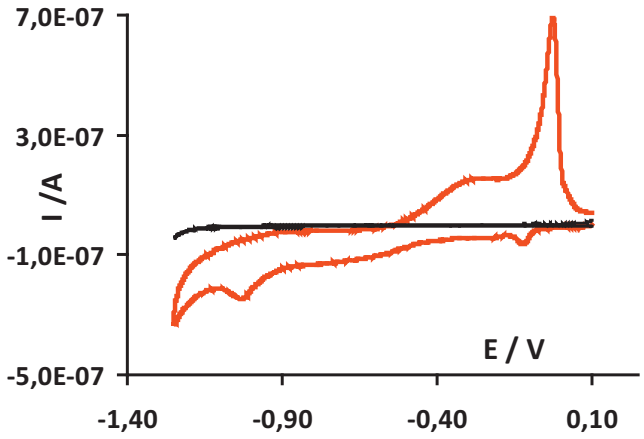

Fig. 6. Cyclic voltammograms of solutions in absence (black) and in presence of vanadium(V) with $[V^V]_{total} = 9.85 \times 10^{-5}$ M (red), for scan rate 80 mV/s. Other voltammetric conditions: $E_i = E_f = 0.10$ V $E_\lambda = -1.20$ V, medium: "buffer" (pH 6.95) and t = (25 ± 1) °C. (For interpretation of the references to colour in this figure legend, the reader is referred to the web version of this article.)

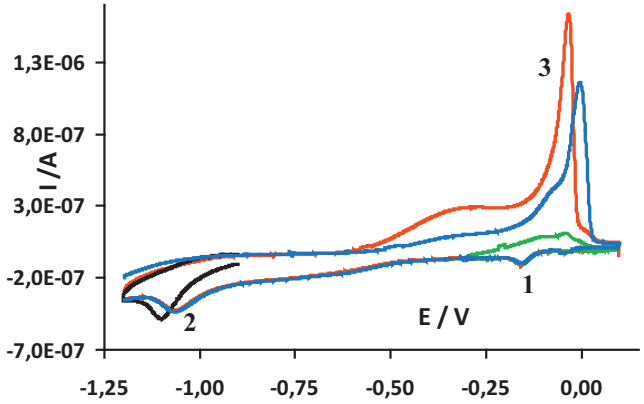

Fig. 7. Cyclic voltammograms of solutions of vanadium(V) with $[V^V]_{total} = 9.85 \times 10^{-5}$ M at different direction of the scan: $E_i = E_f = 0.10$ V and $E_\lambda = -1.20$ V (red); $E_i = E_f = -1.20$ V and $E_\lambda = 0.10$ V (blue); $E_i = E_f = 0.10$ V and $E_\lambda = -0.30$ V (green); $E_i = E_f = -0.90$ V and $E_\lambda = -1.20$ V (black). Other voltammetric conditions: scan rate = 80 mV/s, medium: "buffer" (pH 6.95) and t = (25 ± 1) °C; peak 1: $V^V \rightarrow V^{IV}$ reduction, peak 2: $V^{IV} \rightarrow V^{II}$ reduction, peak 3: $V^{IV} \rightarrow V^V$ oxidation. (For interpretation of the references to colour in this figure legend, the reader is referred to the web version of this article.)

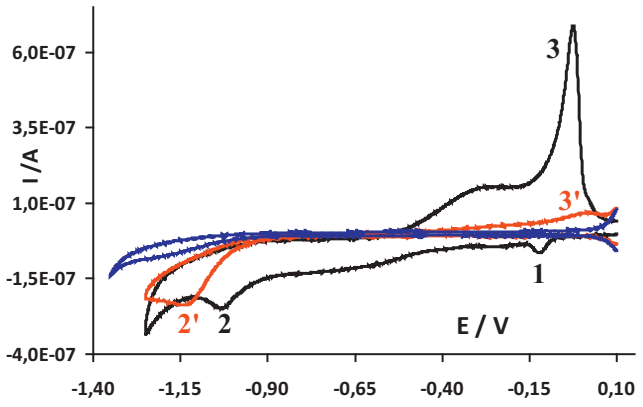

Fig. 8. Cyclic voltammograms of solutions containing vanadate(V) with $[V^V]_{total} = 9.85 \times 10^{-5}$ M in the absence (black) and upon addition of apo-transferrin yielding $[\text{apo-hTF}]_{total}$ (M): red line, 1.21×10^{-5}; blue line, 2.65×10^{-5}. Other voltammetric conditions: $E_i = E_f = 0.10$ V and $E_\lambda = -1.20$ V; scan rate = 80 mV/s; medium: "buffer" (pH 6.95) and t = (25 ± 1) °C. Peak 1: $V^V \rightarrow V^{IV}$ reduction, peak 2 and 2′: $V^{IV} \rightarrow V^{II}$ reduction, peak 3 and 3′: $V^{IV} \rightarrow V^{II}$ oxidation. (For interpretation of the references to colour in this figure legend, the reader is referred to the web version of this article.)

of the proteins and that might be due to apo-hTF and holo-hTF adsorption as non-electroactive species on the mercury surface. To clarify this observation, the adsorption of the proteins alone was analyzed in the same electrolyte medium by AC voltammetry at 90 °angle phase. A decrease of the capacitive current in the region around the potential of zero charge was observed when the proteins were present in solution (data not shown). This clearly demonstrates that adsorption of apo-hTF and holo-hTF occurs on the electrode surface as non-electroactive species. The changes in the background current observed on the CVs upon protein additions means that the proteins prevent the adsorption phenomena observed from solutions containing only vanadium. The peak shift observed on the CVs voltammograms for the second reduction upon additions of apo-hTF or holo-hTF is most probably due to differences in the electrode solution interface, as discussed for Fig. 7, and not a consequence of the complex formation. Therefore, an electrochemical stepwise behavior is still observed for vanadium in the presence of both proteins (apo-hTF and holo-hTF): a quasi-reversible reduction $V^V \rightarrow V^{IV}$ (barely seen for the lowest protein concentrations) with an anodic counterpart, peak 3′, $V^{IV} \rightarrow V^{II}$, followed by the irreversible reduction $V^{IV} \rightarrow V^{II}$, peak 2′. The CV data also shows that apo-hTF and holo-hTF bind to vanadium in both the V^V and V^{IV} states, the complexes being inert, i.e. dissociation does not occur.

The CV data confirm the behavior observed in the DPP experiments. Not only the nature of the redox reactions did not change, nor the

complexation patterns of vanadium with the proteins. This would not necessarily be predictable or expected, since the time window in each technique is different: while in DPP the time parameter (t_p) is $t_p = 0.05$ s, in the CV the time parameter is RT/Fv (s) and for the conditions herein used it corresponds to $0.1 - 3$ s. As a result, in cyclic voltammetry experiments the redox reactions could be reversible and the complexes formed not inert.

3.3. MALDI-TOF experiments

According to the studies of several research groups there is a global agreement in the literature that apo-hTF may bind two $V^{IV}O^{2+}$ moieties in the iron binding sites, this requiring a synergistic anion (normally carbonate) [5] [6] [7] [10] [11] [12] [22] [31] [37] [63]. Additional $V^{IV}O^{2+}$ moieties may possibly bind at other sites, but most probably this does not happen in the biologically relevant concentrations of $V^{IV}O^{2+}$ in blood serum, where the total vanadium concentration is significantly lower than that of hTF [10] [18] [19].

Two sets of MALDI-TOF mass spectra were carried out with samples of apo-hTF and $V^{IV}OSO_4$, with $V^{IV}OSO_4$:apo-hTF molar ratios of 3:1 and 5:1. In the set of experiments with 3:1 M ratio, the average mass of apo-hTF was 79,239 ± 40 Da, and the average mass of samples of $V^{IV}OSO_4$ + apo-hTF samples, was 79,753 ± 40 Da (see e.g. Fig. SI-2-1). Taking into account the different MALDI-TOF mass spectra obtained the difference in masses is ca. 514 ± 40 Da. In the set of experiments with 5:1 M ratio the average masses for the several samples examined slightly differed, but the difference in masses is about the same: 514 ± 40 Da. Therefore, there is a clear and significant increase in mass in the apo-hTF samples containing $V^{IV}OSO_4$, but it is not clear as to how to assign the mass increase. One possibility is to consider the binding of $V^{IV}O^{2+} + SO_4^{2-} + HCO_3^- + H_2O$ at each lobe of apo-hTF, this corresponding to a total mass of 488 Da (see SI section).

Another set of MALDI-TOF mass spectra was carried out with samples of apo-hTF and $NH_4V^VO_3$, with a $NH_4V^VO_3$:apo-hTF molar ratio of 3:1. The average mass of samples of $NH_4V^VO_3$ + apo-hTF samples was 79,416 ± 10 Da (see e.g. Fig. SI-2-2). Taking into account the different MALDI-TOF mass spectra obtained the difference in masses is ca. 177 ± 25 Da; therefore, there is also a clear and significant increase in mass in the apo-hTF samples containing $NH_4V^VO_3$.

The mass of a vanadate(V) anion depends on the number of H_2O molecules assumed to bind to the V atom; for example, assuming the formulation $H_2VO_4^- = V^VO_2(OH^-)_2(H_2O)_3^-$, yields mass = 153 Da. Possible assignments for the mass increase is the binding of one $H_2VO_4^-$ (or HVO_4^{2-}) or of $H_2VO_4^- + NH_4^+$ (or $HVO_4^{2-} + NH_4^+$). The binding of two vanadate(V) moieties would only be consistent with the present MALDI-TOF mass spectra data if each one binds as $V^VO_2^+$ coordinated to several residues of apo-hTF; this corresponds to an increase in mass of ca. 166 Da.

One last set of MALDI-TOF mass spectra was carried out with samples of holo-hTF and $NH_4V^VO_3$, with a $NH_4V^VO_3$:holo-hTF molar ratio of 3:1. The average mass of holo-hTF was 79,725 Da (± 25 Da) (see e.g. Fig. SI-2-3), and the average mass of samples of $NH_4V^VO_3$ + holo-hTF was 80,080 ± 40 Da; Fig. 9 and Fig. SI-2-4 include examples. Again a clear and significant increase in mass occurs in the holo-hTF samples containing $NH_4V^VO_3$, and taking into account the different MALDI-TOF mass spectra obtained we may take: ca. 355 ± 50 Da as reasonable for the difference in masses. Assuming the formulation of $H_2VO_4^-$ as $V^VO_2(OH^-)_2(H_2O)_3^-$ (mass = 153 Da), or of HVO_4^{2-} as $V^VO_2(OH^-)_3(H_2O)_2^{2-}$ (mass = 152 Da), and possible extra binding of NH_4^+ cations, a plausible assignment for the mass increase is the binding of two vanadate(V) anions to holo-hTF.

The matrix used for the MALDI-TOF experiments contains sinapinic acid and the experiments were carried out in a medium containing a NH_4HCO_3 buffer at pH 7.4, but it also contains acetonitrile and a small amount of trifluoroacetic acid. The total masses of apo-hTF and holo-hTF may contain sinapinic acid bound to the proteins and we assume that if this occurs, the number of sinapinic acid molecules bound is equal in the absence or in the presence of vanadium salts. This may not be true and in this case the assignments made for the differences in masses may not be correct. Notwithstanding, the increase in mass observed for the samples of proteins + vanadium salts provides clear evidence of the binding of vanadium(IV) to apo-hTF and vanadate(V) to apo-hTF and holo-hTF.

3.4. Small-angle X-ray scattering (SAXS)

Fig. SI-3-1 shows the experimental SAXS curves from the three apo-hTF samples while the respective derived parameters are summarized in Table 2. The analysis of the data reveals that some properties differ upon metal ion binding but some others are not significantly affected.

The apo-hTF exhibits a radius of gyration of 32.9 Å, relatively close to the one calculated for the apo-hTF + $V^{IV}OSO_4$ (33.1 Å) sample, but slightly different from the value found for apo-hTF + NaV^VO_3 (36.7 Å). Such discrepancies are also detectable in the respective P(r) functions (Fig. 10) which indicate different values of D_{max}, for the three samples. Particularly relevant, apo-hTF + NaV^VO_3 presents a 18 Å larger D_{max} than that determined for the apo-hTF sample, which can probably be explained by the existence of a markedly extended structure; this can be inferred from the P(r) function, which shows an appearance characteristic of elongated structures.

Interestingly, the dimensionless Kratky plot shows that the three samples are not particularly different in terms of their flexibility, indicating a folded globular protein (Fig. SI-3-2). Nevertheless, the plot of apo-hTF + NaV^VO_3 is noticeably different when compared with the other samples.

Finally, the obtained experimental curves were compared with the curve derived from the X-ray structure 2HAV [64]. For the apo-hTF sample, a satisfactory fit was obtained (χ^2 value of 4.3). The metal ion bound samples present worst χ^2 values (28.3 and 17.3) evidencing that $V^{IV}OSO_4$ and NaV^VO_3 alter the overall envelope shape of the protein. The shape reconstruction of the three apo-hTF samples was carried out as shown in Fig. SI-3-3. The Porod volume calculated from the SAXS data is very similar between the apo-hTF and apo-hTF-NaV^VO_3 datasets (143,000 and 145,000 Å^3, respectively), which, when taken with the P(r) function, and the dimensionless Kratky plot suggests some opening or change in the structure upon metal ion binding.

A similar analysis was followed with the three holo-hTF samples (Fig. SI-3-4 and Table 2). As expected, some differences are detectable when compared with the obtained results for apo-hTF, highlighting the different conformation adopted by transferrin according the presence of iron (Fe^{III}).

The obtained Kratky plots reveal that all the holo-hTF samples are folded although not particularly globular (Fig. SI-3-5). It is possible that the samples exposed for SAXS were polydisperse and contained two or more multimerisation states. It could also indicate unusual aggregation behavior; for this study several dilution series were obtained, with the Guinier region being taken from the lowest concentration, however this did not seem to improve data. This is suggested by the poor match between real and reciprocal space radius of gyration, and also the poor agreement at low q between the 3 V83 crystallographic structure [65] and SAXS structure shown in Fig. SI-3-4. At higher q values, less affected by polydispersity or aggregation, the agreement appears to be much better.

Such behavior might account for the changes observed in the parameters derived from the SAXS curves and P(r) functions (Table 2 and Fig. 11) of the three holo-hTF samples and, therefore, no definitive conclusions on protein-ligand interactions can be assumed.

An illustrative example is given by the real space radius of gyration. The obtained value for the holo-hTF sample (40.0 Å) is distinct from those obtained for the holo-hTF + $V^{IV}OSO_4$ (43.7 Å) and holo-hTF + NaV^VO_3 (44.4 Å) samples. Such discrepancy can be interpreted as resulting from the binding of both metal ions to holo-hTF. However, as

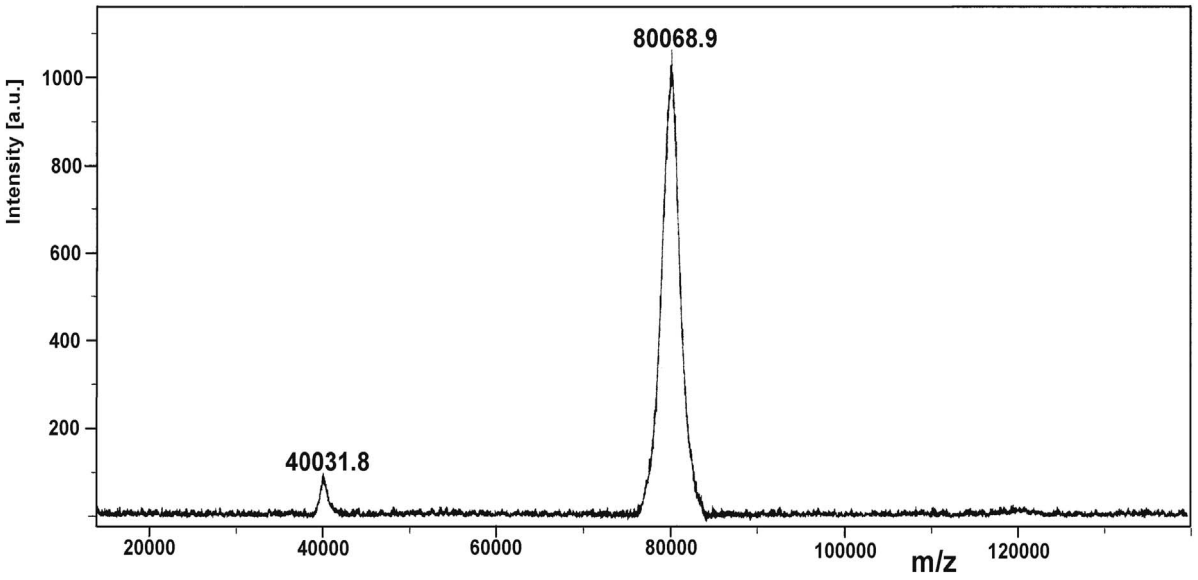

Fig. 9. A MALDI-TOF mass spectrum obtained for samples containing holo-hTF and $NH_4V^VO_3$ with a 3:1 M ratio of $NH_4V^VO_3$:holo-hTF.

Table 2
Structural scattering-derived parameters obtained from the SAXS data collected[a] of apo-hTF, holo-hTF, apo-hTF + $V^{IV}OSO_4$, holo-hTF + $V^{IV}OSO_4$, apo-hTF + NaV^VO_3 and holo-hTF + NaV^VO_3 samples.

	Apo-hTF	Apo-hTF + $V^{IV}OSO_4$	Apo-hTF + NaV^VO_3
R_g (Å) [from Guinier]	32.9	33.1	36.7
R_g (Å) [from P(r)]	32.9	33.1	36.7
D_{max} (Å) [from P(r)]	106	111	124
Porod volume estimate (Å^3)	143,000	130,100	145,000
	Holo-hTF	Holo-hTF + $V^{IV}OSO_4$	Holo-hTF + NaV^VO_3
R_g (Å) [from Guinier]	43.1	55.0	52.9
R_g (Å) [from P(r)]	40.0	43.7	44.4
D_{max} (Å) [from P(r)]	145	153	158
Porod volume estimate (Å^3)	165,000	199,000	194,500

[a] SAXS data collection parameters, obtained at beamline BM29, ESRF: wavelength (Å): 0.99; q range (Å^{-1}): 0.0025–0.5; concentration range (mg/mL): (i) 7.5–0.47 mg/mL (apo-hTF and holo-hTF), (ii) 7.5–0.23 mg/mL (samples containing $V^{IV}OSO_4$), (iii) 4–0.5 mg/mL (samples containing NaV^VO_3); temperature = 25 °C.

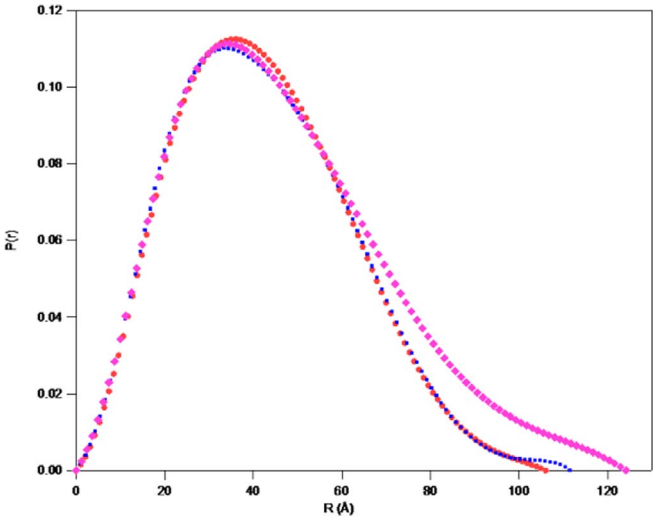

Fig. 10. Pair distance distribution function, P(r), for apo-hTF (red), apo-hTF + $V^{IV}OSO_4$ (blue) and apo-hTF + NaV^VO_3 (pink). (For interpretation of the references to colour in this figure legend, the reader is referred to the web version of this article.)

mentioned, the poor match between these values and the reciprocal space R_g values prevents any detailed and irrefutable assumptions.

In conclusion, the discussed SAXS data suggest that both $V^{IV}OSO_4$ and NaV^VO_3 can effectively interact with human apo-transferrin. Such interaction was particularly detected with vanadate(V) which originated significantly different parameters from those obtained with the apo-hTF sample. In fact, the results indicate a partial closing of apo-hTF upon binding of both V^{IV} and V^V ligands which is less pronounced that that caused by the presence of the Fe^{III} ion in the holo-hTF sample. However, it should be highlighted that the presented SAXS data do not provide evidence supporting the binding mode of the vanadium complexes namely their binding site. Regarding the results from the incubation of human holo-transferrin with both V^{IV} and V^V, considering the discussed potential aggregation, SAXS measurements were not conclusive and no clear evidences supporting the existence or the absence of protein-complex interactions were obtained.

3.5. Possibility of assessment of binding sites

In this work we basically used three types of techniques: electrochemical (Differential Pulse Polarography, Cyclic Voltammetry), MALDI-TOF and SAXS.

Unlike spectroscopy techniques, electroanalytical techniques are not normally suitable to provide information about structure. Voltammetry gives information about the electrochemical behavior of a given compound, namely of metal ions, as is the case here. Nevertheless, depending on medium conditions, changes in the electron-transfer might occur as a consequence of the interactions in solution between the electroactive species and other molecules, namely due to complexation. From the changes in the relationship between potential and current information of parameters not only representative of solution thermodynamic equilibria but also on kinetic factors such as the lability of the complexes, is provided. The V-protein complexes formed are non-labile and non-electroactive over the potential range studied and only non-protein bound vanadium ions are electroactive.

Regarding MALDI-TOF mass spectrometry, we only obtain difference in masses between samples containing only the proteins or the protein + complexes. Therefore, it is not possible to directly access the specific sites with this technique.

Regarding SAXS, the technique allows obtaining a global model of

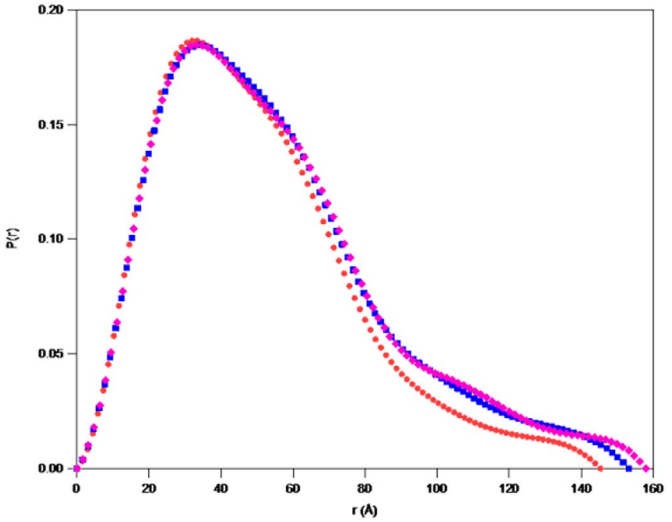

Fig. 11. Pair distance distribution function, P(r), for holo-hTF (red), holo-hTF + $V^{IV}OSO_4$ (blue) and holo-hTF + $NaV^{V}O_3$ (pink). (For interpretation of the references to colour in this figure legend, the reader is referred to the web version of this article.)

the protein with low resolution, where significant conformational changes induced by the compounds may be detected. However, the binding sites cannot be accessed (in a direct way). Assuming that the open conformation of apo-hTF corresponds to the SAXS profile of native apo-hTF, and that the closed conformation corresponds to the SAXS profile of native holo-hTF, it is possible to state that, considering the parameters obtained, the binding of V^{IV} and V^{V} to apo-hTF changes the conformation of the protein that gets closer to the closed conformation of hTF, but however does not get to the fully closed conformation. However, this does not allow to safely conclude that this corresponds to a distinct binding mode. In the case of holo-hTF it is reasonable to assume/expect that the binding site is at or close to the surface of the protein, but this does not mean that the same occurs with apo-hTF. Noteworthy is the fact that, at least in the system $V^{IV}O$-apo-hTF, several studies of several groups (circular dichroism and EPR) indicated that the binding of $V^{IV}O$ takes place at the iron binding sites [5] [6] [7] [8] [9] [10] [11] [12] [14] [22].

4. Conclusions

The electrochemical behavior of solutions containing vanadate(V) at pH = 7.0 ± 0.1, analyzed by using two different voltammetric techniques at a mercury electrode: DPP and CV, with different time windows, is consistent with a stepwise reduction of $V^{V} \rightarrow V^{IV}$ and $V^{IV} \rightarrow V^{II}$. The first is a quasi-reversible process, while the second is an irreversible process, most probably due to the irreversible redox reaction of $V^{IV} \rightarrow V^{II}$ ions on a mercury electrode. All attempts to observe the reduction of V^{IV} to V^{III} using different types of electrodes were not successful.

In the presence of apo-hTF or holo-hTF, the behavior of vanadium in DPP remains essentially the same, the stepwise reduction $V^{V} \rightarrow V^{IV}$ and $V^{IV} \rightarrow V^{II}$ occurring again. However, it is clear from the electrochemical data that vanadium binds to both proteins. Peak potentials remain the same within the experimental error, but the peak currents decrease with the increase of the protein concentration in solution. This behavior is consistent with the formation of electrochemically inert protein-vanadium complexes, meaning that dissociation does not occur during the electrochemical measurement. The complexes are also non-electroactive since no other voltammetric signals were detected in the potential range studied. Both peak current intensities are affected upon protein addition, thus the reduction does not destroy the complexes formed with vanadium(V). Accordingly, treatment of the voltammetric data using either the reduction $V^{V} \rightarrow V^{IV}$ and/or the reduction $V^{IV} \rightarrow V^{II}$, was consistent, in the experimental conditions used, with the formation of 2:1 complexes in the case of the system V^{V}-apo-hTF and a mixture 1:1 and 2:1 complexes in the case of the V^{V}-holo-hTF system. In the V^{V}-apo-hTF system the conditional formation constant of log $K'_{(V)2(apo\text{-}hTF)}$ (or β'_2) = 10.2 ± 0.4, is reasonably similar to those obtained at pH = 7.4 by Kiss and co-workers (= 11.5) [8] and Harris and Carrano [33] (~11.5). For the V^{V}-holo-hTF system the $\log K'_{(V)1(holo\text{-}hTF)}$ = 4.3 ± 0.5 and $\log K'_{(V)2(holo\text{-}hTF)}$ (or β'_2) = 8.3 ± 0.6 were determined.

The observations made in the presence of the proteins by CV are in agreement with those made by DPP and corroborate, in a qualitative way, the conclusions mentioned above. No intermediate oxidation states of vanadium or complexes with different lability were detected. Moreover, adsorption phenomena due to negatively charged vanadium species in solution at potentials close to the reduction potential of V^{V} to V^{IV} were quite evident, in particularly in the CV data. The use of suitable diagnosis tests and properly designed experiments were fundamental to analyze the voltammetric data correctly.

MALDI-TOF mass spectrometric data were obtained for samples of $NH_4V^{V}O_3$ with both apo-hTF and holo-hTF, and $V^{IV}OSO_4$ with apo-hTF, using V:hTF ratios of 3:1. In all cases the increase in the mass are consistent with the binding of vanadium to the proteins. Moreover, the discussed SAXS data suggest that both $V^{IV}OSO_4$ and $NaV^{V}O_3$ can effectively interact with human apo-transferrin; on the other hand, regarding holo-hTF, the SAXS measurements were not conclusive and no clear evidences were obtained supporting the existence or the absence of protein-ligand interactions. In fact, the data suggests that the conformation of holo-hTF does not change in the presence of either $V^{IV}OSO_4$ or $NH_4V^{V}O_3$.

Previous studies globally agree that in the blood serum vanadium binds and is transported mainly by transferrin [12]. For the concentrations normally found in the blood of humans treated with vanadium compounds ca. up to 1–5 μM [18] [19], vanadium is bound to hTF not including the carrier ligand. As found in this work and reported elsewhere [37] oxidovanadium(IV) binds holo-hTF. On the other hand $V^{IV}O^{2+}$ is very unstable towards aerobic oxidation to V^{V} and vanadate (V) has been shown to bind apo-hTF and there are reports that it may also bind to holo-hTF [31] [33]. The present work provides additional evidence for the binding of vanadium in both oxidation states to these proteins, and electrochemical data allowed estimation of conditional binding constants of V^{V} to holo-hTF and apo-hTF. Noteworthy is the fact that since this binding possibly does not affect the conformation of holo-hTF, the protein is most probably still recognized by the cell transferrin receptors. Therefore, it is anticipated that V^{IV} or V^{V} bound to holo-hTF may be efficiently up-taken by the cells through the receptor-mediated endocytosis of hTF.

Abbreviations

EPR	Electron paramagnetic resonance
HSA	Human serum albumin
Apo-hTF	Human serum apo-transferrin
Holo-hTF	Human serum holo-transferrin
CD	Circular dichroism
DDAB	Didodecyldimethylammonium bromide
ACV	Alternating current voltammetry
CV	Cyclic Voltammetry
DPP	Differential Pulse Polarography
DPV	Differential Pulse voltammetry
K'	Conditional formation constant (only valid for specified experimental conditions)
MALDI-TOF	Matrix-assisted laser desorption/ionization time-of-flight
SAXS	Small-angle X-ray scattering
t_p	Time parameter

Acknowledgements

This work was supported by Fundação para a Ciência e Tecnologia (FCT), Portugal (projects UID/Multi/04349/2013, UID/QUI/00100/2013, RECI/QEQ-QIN/0189/2012, RECI/QEQMED/0330/2012, PTDC/QEQ-MED/1902/2014 and grants SFRH/BD/77894/2011 and BPD/CQE-2017-029 to M.F.A.S) and programme FCT Investigator: IF/00100/2013 (I.C.) and IF/00007/2015 (H.M.S.). The PROTEOMASS Scientific Society is acknowledged by the funding provided to the Biological Mass Spectrometry *Isabel Moura*. J.L.C., M.F.A.S., L.F., H.M.S. and T.S.S. acknowledge the funding provided by Unidade de Ciências Biomoleculares Aplicadas - UCIBIO, (UID/Multi/04378/2013) and co-financed by the ERDF under the PT2020 Partnership Agreement (POCI-01-0145-FEDER-007728). H.M.S. and J.L.C. also acknowledge the Associate Laboratory for Green Chemistry LAQV (UID/QUI/50006/2013) and co-financed by the ERDF under the PT2020 Partnership Agreement (POCI-01-0145-FEDER-007265). The authors would also like to thank the staff of ESRF and of EMBL (Grenoble, France) for assistance and support in collecting the SAXS data at beamline BM29.

Appendix A. Supplementary data

Supplementary data to this article can be found online at https://doi.org/10.1016/j.jinorgbio.2017.12.012.

References

[1] H.Z. Sun, H.Y. Li, P.J. Sadler, Chem. Rev. 99 (1999) 2817–2842.
[2] E.E. Battin, A. Lawhon, J.L. Brumaghim, D.H. Hamilton, J. Chem. Educ. 86 (2009) 969–972.
[3] C.D. Quarles, J.L. Brumaghim, R.K. Marcus, Metallomics 2 (2010) 154–161.
[4] R.W. Evans, X.L. Kong, R.C. Hider, Biochim. Biophys. Acta, Gen. Subj. 1820 (2012) 282–290.
[5] T. Kiss, T. Jakusch, D. Hollender, A. Dornyei, E.A. Enyedy, J.C. Pessoa, H. Sakurai, A. Sanz-Medel, Coord. Chem. Rev. 252 (2008) 1153–1162.
[6] T. Jakusch, D. Hollender, E.A. Enyedy, C.S. Gonzalez, M. Montes-Bayon, A. Sanz-Medel, J.C. Pessoa, I. Tomaz, T. Kiss, Dalton Trans. (2009) 2428–2437.
[7] D. Sanna, G. Micera, E. Garribba, Inorg. Chem. 49 (2010) 174–187.
[8] T. Jakusch, A. Dean, T. Oncsik, A.C. Benyei, V. Di Marco, T. Kiss, Dalton Trans. 39 (2010) 212–220.
[9] D. Sanna, L. Biro, P. Buglyo, G. Micera, E. Garribba, J. Inorg. Biochem. 115 (2012) 87–99.
[10] J.C. Pessoa, I. Tomaz, Curr. Med. Chem. 17 (2010) 3701–3738.
[11] J.C. Pessoa, S. Etcheverry, D. Gambino, Coord. Chem. Rev. 301–302 (2015) 24–48.
[12] J.C. Pessoa, E. Garribba, M.F.A. Santos, T. Santos-Silva, Coord. Chem. Rev. 301–302 (2015) 49–86.
[13] T.C. Delgado, A.I. Tomaz, I. Correia, J.C. Pessoa, J.G. Jones, C.F.G.C. Geraldes, M.M.C.A. Castro, J. Inorg. Biochem. 99 (2005) 2328–2339.
[14] D. Sanna, M. Serra, G. Micera, E. Garribba, Inorg. Chem. 53 (2014) 1449–1464.
[15] A. Levina, A.I. McLeod, S.J. Gasparini, A. Nguyen, W.G.M. De Silva, J.B. Aitken, H.H. Harris, C. Glover, B. Johannessen, P.A. Lay, Inorg. Chem. 54 (2015) 7753–7766.
[16] J.C. Pessoa, I. Tomaz, T. Kiss, P. Buglyo, J. Inorg. Biochem. 84 (2001) 259–270.
[17] J.C. Pessoa, I. Tomaz, T. Kiss, E. Kiss, P. Buglyo, J. Biol. Inorg. Chem. 7 (2002) 225–240.
[18] K.H. Thompson, C. Orvig, J. Inorg. Biochem. 100 (2006) 1925–1935.
[19] K.H. Thompson, J. Lichter, C. Lebel, M.C. Scaife, J.H. McNeill, C. Orvig, J. Inorg. Biochem. 103 (2009) 554–558.
[20] T. Jakusch, J.C. Pessoa, T. Kiss, Coord. Chem. Rev. 255 (2011) 2218–2226.
[21] J.C. Pessoa, J. Inorg. Biochem. 147 (2015) 4–24.
[22] D. Sanna, V. Ugone, M. Serra, E. Garribba, J. Inorg. Biochem. 173 (2017) 52–65.
[23] I. Correia, I. Chorna, I. Cavaco, S. Roy, M.L. Kuznetsov, N. Ribeiro, G. Justino, F. Marques, T. Santos-Silva, M.F.A. Santos, M.S. Hugo, J.L. Capelo, J. Doutch, J.C. Pessoa, Chem. Asian. J. 12 (2017) 2062–2084.
[24] D. Sanna, V. Ugone, G. Micera, P. Buglyo, L. Biro, E. Garribba, Dalton Trans. 46 (2017) 8950–8967.
[25] N.D. Chasteen, J.K. Grady, C.E. Holloway, Inorg. Chem. 25 (1986) 2754–2760.
[26] L. Pettersson, I. Andersson, A. Gorzsas, Coord. Chem. Rev. 237 (2003) 77–87.
[27] D. Rehder, Bioinorganic Vanadium Chemistry, John Wiley & Sons, Ltd, Chichester, 2008.
[28] A. Tracey, G.R. Willsky, E.S. Takeuchi, Vanadium: Chemistry, Biochemistry, Pharmacology and Practical Applications, CRC Press, Boca Raton, 2007.
[29] L.F. Vilas Boas, J. Costa Pessoa, Comprehensive coordination chemistry, in: G. Wilkinson, R.D. Gillard, J.A. McCleverty (Eds.), Vanadium, Chapter 33, vol. 3, Pergamon, Oxford, 1987, pp. 453–583.
[30] L. Alderighi, P. Gans, A. Lenco, D. Peters, A. Sabatini, A. Vacca, Coord. Chem. Rev. 184 (1999) 311–318.
[31] J.C. Pessoa, G. Goncalves, S. Roy, I. Correia, S. Mehtab, M.F.A. Santos, T. Santos-Silva, Inorg. Chim. Acta 420 (2014) 60–68.
[32] W.R. Harris, Biochemistry 24 (1985) 7412–7418.
[33] W.R. Harris, C.J. Carrano, J. Inorg. Biochem. 22 (1984) 201–218.
[34] A.K. Bordbar, A.L. Creagh, F. Mohammadi, C.A. Haynes, C. Orvig, J. Inorg. Biochem. 103 (2009) 643–647.
[35] G. Heinemann, B. Fichtl, M. Mentler, W. Vogt, J. Inorg. Biochem. 90 (2002) 38–42.
[36] A. Butler, H. Eckert, J. Am. Chem. Soc. 111 (1989) 2802–2809.
[37] D. Sanna, G. Micera, E. Garribba, Inorg. Chem. 52 (2013) 11975–11985.
[38] I. Bertini, G. Canti, C. Luchinat, Inorg. Chim. Acta - Bioinorg. 67 (1982) L21–L23.
[39] I. Bertini, C. Luchinat, L. Messori, J. Inorg. Biochem. 25 (1985) 57–60.
[40] M.H. Nagaoka, T. Yamazaki, T. Maitani, Biochem. Biophys. Res. Commun. 296 (2002) 1207–1214.
[41] A. Levina, A.I. McLeod, L.E. Kremer, J.B. Aitken, C.J. Glover, B. Johannessen, P.A. Lay, Metallomics 6 (2014) 1880–1888.
[42] J.J. Lingane, J. Am. Chem. Soc. 67 (1945) 182–188.
[43] I.M. Kolthoff, Polarography, 2nd edition, Interscience Publishers, New York, 1952.
[44] M.J. Shaw, Vanadium electrochemistry, in: A.J. Bard, M. Stratmann, F. Scholz, C.J. Pickett (Eds.), Encyclopedia of Electrochemistry, vol. 7, Wiley-VCH, 2006, pp. 357–381.
[45] P. Galloni, V. Conte, B. Floris, Coord. Chem. Rev. 301 (2015) 240–299.
[46] H.H. Cai, J. Cai, P.H. Yang, Bioorg. Med. Chem. Lett. 19 (2009) 863–866.
[47] M. Guo, L. He, P.J. Strong, H.L. Wang, Chemosphere 112 (2014) 472–480.
[48] D.H. Hamilton, I. Turcot, A. Stintzi, K.N. Raymond, J. Biol. Inorg. Chem. 9 (2004) 936–944.
[49] P. Pernot, A. Round, R. Barrett, A.D. Antolinos, A. Gobbo, E. Gordon, J. Huet, J. Kieffer, M. Lentini, M. Mattenet, C. Morawe, C. Mueller-Dieckmann, S. Ohlsson, W. Schmid, J. Surr, P. Theveneau, L. Zerrad, S. McSweeney, J. Synchrotron Radiat. 20 (2013) 660–664.
[50] A. Round, F. Felisaz, L. Fodinger, A. Gobbo, J. Huet, C. Villard, C.E. Blanchet, P. Pernot, S. McSweeney, M. Roessle, D.I. Svergun, F. Cipriani, Acta Crystallogr. D Biol. Crystallogr. 71 (2015) 67–75.
[51] M.V. Petoukhov, D. Franke, A.V. Shkumatov, G. Tria, A.G. Kikhney, M. Gajda, C. Gorba, H.D.T. Mertens, P.V. Konarev, D.I. Svergun, J. Appl. Crystallogr. 45 (2012) 342–350.
[52] D. Svergun, C. Barberato, M.H.J. Koch, J. Appl. Crystallogr. 28 (1995) 768–773.
[53] R.P. Rambo, J.A. Tainer, Biopolymers 95 (2011) 559–571.
[54] D. Franke, D.I. Svergun, J. Appl. Crystallogr. 42 (2009) 342–346.
[55] V.V. Volkov, D.I. Svergun, J. Appl. Crystallogr. 36 (2003) 860–864.
[56] D.I. Svergun, Biophys. J. 76 (1999) 2879–2886.
[57] R.L. Birke, M.H. Kim, M. Strassfeld, Anal. Chem. 53 (1981) 852–856.
[58] A.J. Bard, L.R. Faulkner, Electrochemical Methods, Fundamentals and Applications, 2nd ed., John Wiley & Sons, New York, 2001.
[59] M. Lovric, J. Electroanal. Chem. 218 (1987) 77–91.
[60] M.M.C. Santos, A.M. Mota, Trace metal speciation of labile chemical species in natural water: electrochemical methods, chapter 5, in: A. Tessier, D.R. Turner (Eds.), Metal Speciation and Bioavailability in Aquatic Systems, Wiley, Chichester, 1995.
[61] J.B. Vincent, S. Love, Biochim. Biophys. Acta, Gen. Subj. 1820 (2012) 362–378.
[62] R.H. Wopschall, I. Shain, Anal. Chem. 39 (1967) 1514.
[63] S. Mehtab, G. Goncalves, S. Roy, A.I. Tomaz, T. Santos-Silva, M.F.A. Santos, M.J. Romao, T. Jakusch, T. Kiss, J.C. Pessoa, J. Inorg. Biochem. 121 (2013) 187–195.
[64] J. Wally, P.J. Halbrooks, C. Vonrhein, M.A. Rould, S.J. Everse, A.B. Mason, S.K. Buchanan, J. Biol. Chem. 281 (2006) 24934–24944.
[65] N. Noinaj, N.C. Easley, M. Oke, N. Mizuno, J. Gumbart, E. Boura, A.N. Steere, O. Zak, P. Aisen, E. Tajkhorshid, R.W. Evans, A.R. Gorringe, A.B. Mason, A.C. Steven, S.K. Buchanan, Nature 483 (2012) 53–U92.